

Synthesis, cytotoxic activity and DNA interaction studies of new dinuclear platinum(II) complexes with aromatic 1,5-naphthyridine bridging ligand: DNA binding mode of polynuclear platinum(II) complexes in relation to the complex structure

Bata Konovalov^a, Marija D. Živković^b, Jelena Z. Milovanović^c, Dragana B. Djordjević^c, Aleksandar N. Arsenijević^c, Ivana R. Vasić^b, Goran V. Janjić^d, Andjela Franich^a, Dragan Manojlović^{e,f}, Sandra Skrivanj^e, Marija Z. Milovanović^c, Miloš I. Djuran^g, Snežana Rajković^{*a}

^a*University of Kragujevac, Faculty of Science, Department of Chemistry, R. Domanovića 12, 34000 Kragujevac, Serbia, E-mail: snezana@kg.ac.rs*

^b*University of Kragujevac, Faculty of Medical Sciences, Department of Pharmacy, Svetozara Markovića 69, 34000 Kragujevac, Serbia*

^c*University of Kragujevac, Faculty of Medical Sciences, Department of Microbiology and immunology, Center for Molecular Medicine and Stem Cell Research, Svetozara Markovića 69, 34000 Kragujevac, Serbia*

^d*University of Belgrade, Institute of Chemistry, Metallurgy and Technology, Njegoševa 12, 11000 Belgrade, Serbia*

^e*University of Belgrade, Faculty of Chemistry, Studentskitrg 12-16, 11000 Belgrade, Serbia*

^f*South Ural State University, Lenin prospekt 76, 454080 Chelyabinsk, Russia*

^g*Serbian Academy of Sciences and Arts, Knez Mihailova 35, 11000 Belgrade, Serbia*

*Corresponding author. Tel.: +381 34 300 251; fax: +381 34 335 040 (S. Rajković)

E-mail address: snezana@kg.ac.rs (S. Rajković).

Abstract

The synthesis, spectroscopic characterization, cytotoxic activity and DNA binding evaluation of seven new dinuclear platinum(II) complexes **Pt1–Pt7**, with general formula $[\{\text{Pt}(\text{L})\text{Cl}\}_2(\mu\text{-1,5-nphe})](\text{ClO}_4)_2$ (1,5-nphe is 1,5-naphthyridine; while L is two amines (**Pt1**) or one bidentate coordinated diamine: ethylenediamine (**Pt2**), (\pm)-1,2-propylenediamine (**Pt3**), *trans*-(\pm)-1,2-diaminocyclohexane (**Pt4**), 1,3-propylenediamine (**Pt5**), 2,2-dimethyl-1,3-propylenediamine (**Pt6**), and 1,3-pentanediamine (**Pt7**)), were reported. *In vitro* cytotoxic activity of these complexes was evaluated against three tumor cell lines, murine colon carcinoma (CT26), murine mammary carcinoma (4T1) and murine lung cancer (LLC1) and two normal cell lines, murine mesenchymal stem cells (MSC) and human fibroblasts (MRC-5) cells. The results of MTT assay indicate that all investigated complexes have almost no cytotoxic effects on 4T1 and very low cytotoxicity toward LLC1 cell lines. In contrast to the effects on LLC1 and 4T1 cells, complexes **Pt1** and **Pt2** had significant cytotoxic activity toward CT26 cells. Complex **Pt1** had much lower IC_{50} value for activity on CT26 cells compared with cisplatin. In comparison to cisplatin, all dinuclear **Pt1–Pt7** complexes showed lower cytotoxicity toward normal MSC and MRC-5 cells. In order to measure the amount of the platinum(II) complexes taken up by the cells, we quantified the cellular platinum content using inductively coupled plasma mass spectrometry (ICP-QMS). Molecular docking study, performed to evaluate the potential binding mode of dinuclear platinum(II) complexes **Pt1–Pt7** and their aqua derivatives **W1–W7**, respectively, at double stranded DNA was shown that groove spanning and backbone tracking are the most stable binding modes.

Keywords: Dinuclear platinum(II) complexes; 1,5-naphthyridine; Cytotoxicity; Molecular docking; DNA interaction

Table of Contents

Table S1 NMR (^1H and ^{13}C) chemical shifts (δ , ppm), together with multiplicities and coupling constants ($J_{\text{H-H}}$, Hz), for the free 1,5-naphthyridine and the corresponding 1,5-naphthyridine-bridged Pt(II) complexes Pt1–Pt7 in D_2O as solvent with TSP as the internal standard.	S6
Table S2 The amounts ($\mu\text{g/g}$) of platinum taken up by the LLC1 cells after 2 h of treatment at 37 °C with dinuclear Pt1–Pt7 complexes and cisplatin at 2 μM in DMSO medium determined by using inductively coupled plasma mass spectrometry (ICP-QMS). The results represent the mean value of six replicate measurements. The correlation coefficient of the regression line was 1.0000.	S7
Table S3 Optimized operating conditions of ICP-QMS.	S7
Fig. S1 Illustrations of covalent DNA binding modes in crystal structures, extracted from PDB. The ligand is shown by ball&stick style.	S8
Fig. S2 Illustrations of groove binding and intercalation of ligands on DNA in crystal structures, extracted from PDB. The ligand is shown by ball&stick style.	S9
Fig. S3 Illustrations of backbone tracking of ligands on DNA in crystal structures, extracted from PDB. The ligand is shown by ball&stick style.	S10
Fig. S4 UV–vis spectra of the investigated dinuclear platinum(II) complexes Pt1–Pt7 measured in $5 \cdot 10^{-5}$ M water solution.	S11
Fig. S5 Representative graphs of 4T1, CT26, and LLC1 cell survival after 72 h cell growth in the presence of the platinum(II) complexes and cisplatin.	S12
Fig. S6 The structures of the most stable binding modes of dinuclear platinum(II) complexes (Pt1–Pt7) to iron-free (apo) form of the recombinant N-lobe of human serum transferrin (ApoTfN), as assessed by molecular docking.	S13
Fig. S7 Amino-acid environment of Pt1–Pt7 complexes in the most stable	S14

orientation of these complexes and iron-free (apo) form of the recombinant N-lobe of human serum transferrin (ApoTfN), as assessed by molecular docking.

Fig. S8 Absorption spectra of **Pt2** and **Pt5** complexes in the absence and in **S15** the presence of increasing amounts of CT-DNA measured in 0.01 M phosphate buffer solution (PBS) at pH 7.40 and 37 °C. $c(\text{Pt(II) complex}) = 8 \mu\text{M}$ ($r = c(\text{DNA})/c(\text{Pt(II) complex}) = 0, 0.1, 0.6, 1.0, 1.6, 2.0$). Arrow shows the absorption intensity changes upon increasing of CT-DNA concentration.

Fig. S9 Emission spectra of the CT-DNA-EtBr system in the absence and in **S16** the presence of increasing amounts of **Pt2** and **Pt5** complexes. The spectra were measured in 0.01 M in phosphate buffer solution at pH 7.40 and room temperature. $c(\text{EtBr}) = 8 \mu\text{M}$; $c(\text{DNA}) = 8 \mu\text{M}$; $c(\text{Pt(II) complex}) = (0-8) \mu\text{M}$; $\lambda_{\text{ex}} = 527 \text{ nm}$. Arrow shows the emission intensity changes upon increasing of the complex concentration.

Fig. S10 Binding environments for the most stable binding of aqua complexes **W1** **S17** and **W2** to DNA, as assessed by molecular docking (**W1** and **W2** represent aqua derivatives of the corresponding chloride platinum(II) complexes **Pt1** and **Pt2**, respectively).

Fig. S11 Binding environments for the most stable binding of aqua complexes **W3** **S17** and **W4** to DNA, as assessed by molecular docking (**W3** and **W4** represent aqua derivatives of the corresponding chloride platinum(II) complexes **Pt3** and **Pt4**, respectively).

Fig. S12 Binding environments for the most stable binding of aqua complexes **W5** **S18** and **W6** to DNA, as assessed by molecular docking (**W5** and **W6** represent aqua derivatives of the corresponding chloride platinum(II) complexes **Pt5** and **Pt6**,

respectively).

Fig. S13 Two the most stable binding modes and binding environment for the most **S18**
stable binding mode of platinum(II)-aqua complex **W7** to DNA (backbone
tracking), as assessed by molecular docking (**W7** represents aqua derivative of the
corresponding chloride platinum(II) complex **Pt7**).

Fig. S14 The structures of the most stable binding modes of dinuclear platinum(II) **S19**
complexes **Pt1–Pt7** to DNA, as assessed by molecular docking.

Scheme S1 Reaction pathway for preparation of dinuclear platinum(II) complexes **S20**
Pt1–Pt7 (L is 2NH₃ or bidentate coordinated diamine ligand: en, 1,2-pn, dach, 1,3-
pd, 2,2-diMe-1,3-pd and 1,3-pnd; 1,5-nphe is 1,5-naphthyridine).

Scheme S2 Molecular structures of some polynuclear platinum(II) complexes, **S20**
mentioned in the main body of the manuscript.

Table 1 NMR (^1H and ^{13}C) chemical shifts (δ , ppm), together with multiplicities and coupling constants ($J_{\text{H-H}}$, Hz), for the free 1,5-naphthyridine and the corresponding 1,5-naphthyridine-bridged Pt(II) complexes **Pt1–Pt7** in D_2O as solvent with TSP as the internal standard.

Ligand/ Complex	NMR assignments						
	^1H			^{13}C			
	H2, H6	H4, H8	H3, H7	C2, C6	C4, C8	C3, C7	C4a, C8a
1,5-nphe	8.57 <i>dd</i> ; J= 4.3, 1.4	7.91 <i>d</i> ; J=7.4	7.48 <i>dd</i> ; J= 8.6, 4.3	153.6	137.7	127.8	142.8
Pt1	10.38 <i>d</i> ; J= 8.6	9.69 <i>d</i> ; J=5.3	8.24 <i>dd</i> ; J= 9.0, 5.4	161.4	147.4	130.5	147.5
Pt2	10.25 <i>d</i> J=8.7	9.61 <i>d</i> ; J=5.1	8.17 <i>m</i>	159.6	141.4	129.0	147.6
Pt3	10.22 <i>d</i> J=8.6	9.58 <i>m</i>	8.16 <i>d</i> ; J=7.6	161.0	142.9	130.3	147.5
Pt4	10.23 <i>m</i>	9.58 <i>m</i>	8.16 <i>m</i>	161.7	142.2	130.2	147.2
Pt5	10.27 <i>d</i> ; J=9.1	9.58 <i>d</i> ; J=5.7)	8.18 <i>m</i>	161.2	142.3	130.4	148.0
Pt6	10.27 <i>d</i> ; J=8.9	9.57 <i>d</i> ; J=5.1	8.16 <i>dd</i> ; J=9.0, 5.1	161.0	142.3	130.5	148.4
Pt7	10.23 <i>m</i>	9.58 <i>m</i>	8.17 <i>m</i>	161.1	142.6	130.4	147.6

s = singlet; *d* = doublet; *dd* = doublet of doublets; *m* = multiplet

Table S2 The amounts ($\mu\text{g/g}$) of platinum taken up by the LLC1 cells after 2 h of treatment at 37 °C with dinuclear **Pt1–Pt7** complexes and cisplatin at 2 μM in DMSO medium determined by using inductively coupled plasma mass spectrometry (ICP-QMS). The results represent the mean value of six replicate measurements. The correlation coefficient of the regression line was 1.0000.

Complex	Concentration of platinum ($\mu\text{g/g}$)	
	Mean	St. Dev.
Pt1	4.23	0.07
Pt2	6.52	0.10
Pt3	1.51	0.03
Pt4	1.51	0.04
Pt5	4.94	0.07
Pt6	1.20	0.03
Pt7	1.05	0.02
cisplatin	0.72	0.02
untreated	0.01	0.01

Table
operating
ICP-QMS.

S3

Optimized
conditions of

Instrument parameter	Operating condition
Forward power (W)	1550
Ar gas flow rates (L/min)	
Coolant	0.80
Auxiliary	1.13
Transport gas	14
Spray chamber	Glass cyclonic
Nebulizer	PFA-ST MicroFlow
Dwell time(s)	0.01
Number of Channels	1
Spacing	0.1
Resolutin	Resolutin
Replicates	6

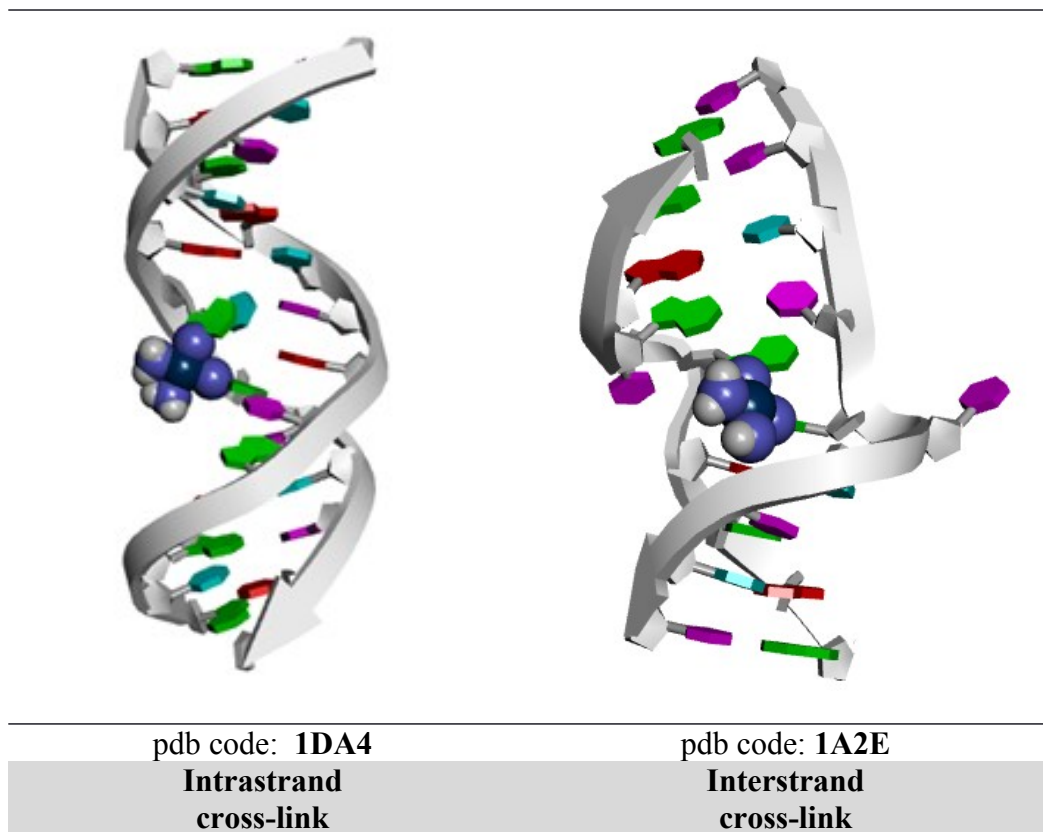


Fig. S1 Illustrations of covalent DNA binding modes in crystal structures, extracted from PDB. The ligand is shown by ball&stick style.

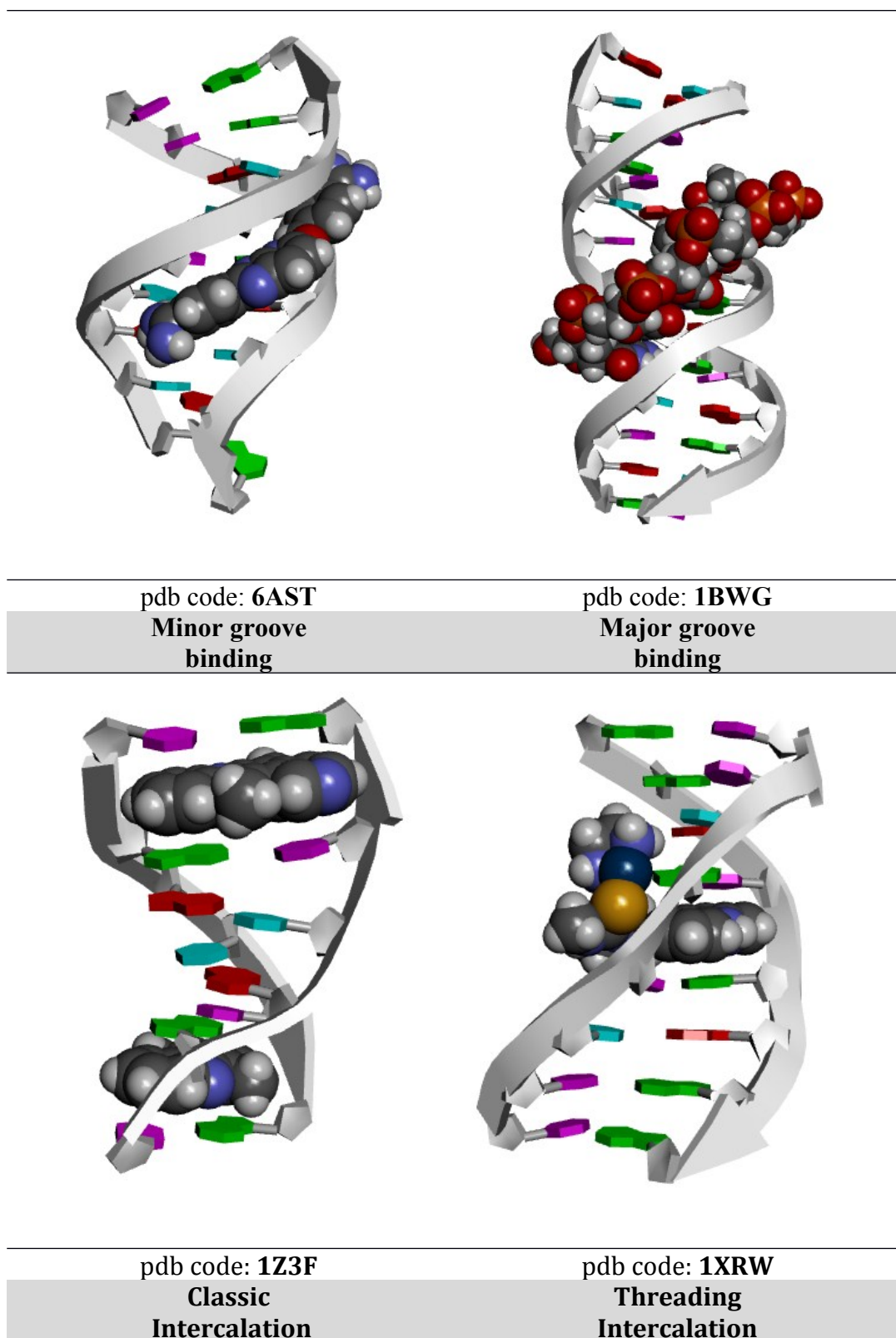
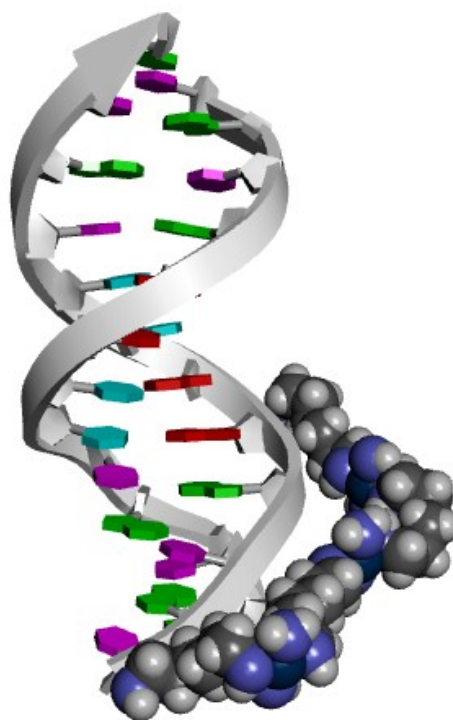


Fig. S2 Illustrations of groove binding and intercalation of ligands on DNA in crystal structures, extracted from PDB. The ligand is shown by ball&stick style.



pdb code: **2DYW**

Fig. S3 Illustrations of backbone tracking of ligands on DNA in crystal structures, extracted from PDB. The ligand is shown by ball&stick style.

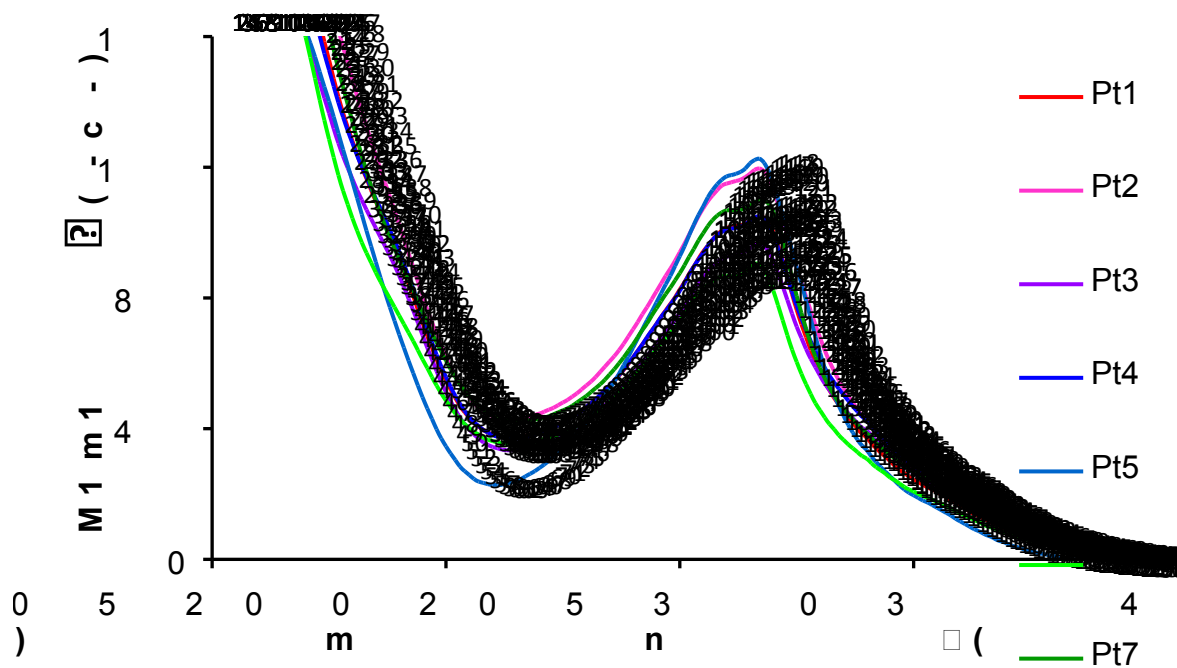


Fig. S4 UV-vis spectra of the investigated dinuclear platinum(II) complexes **Pt1–Pt7** measured in $5 \cdot 10^{-5}$ M water solution.

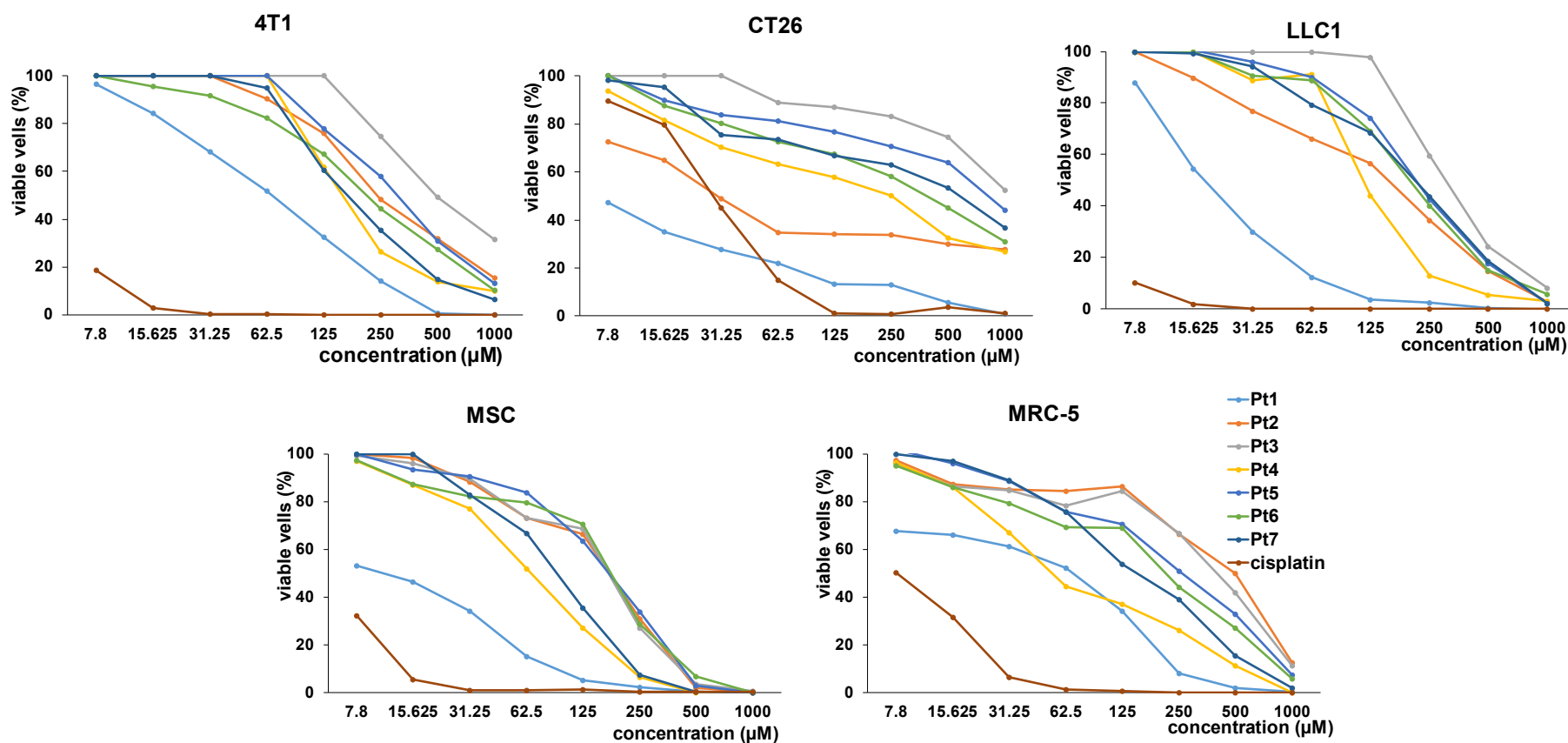


Fig. S5 Representative graphs of 4T1, CT26, LLC1, MSC and MRC-5 cell survival after 72 h cell growth in the presence of the platinum(II) complexes and cisplatin.

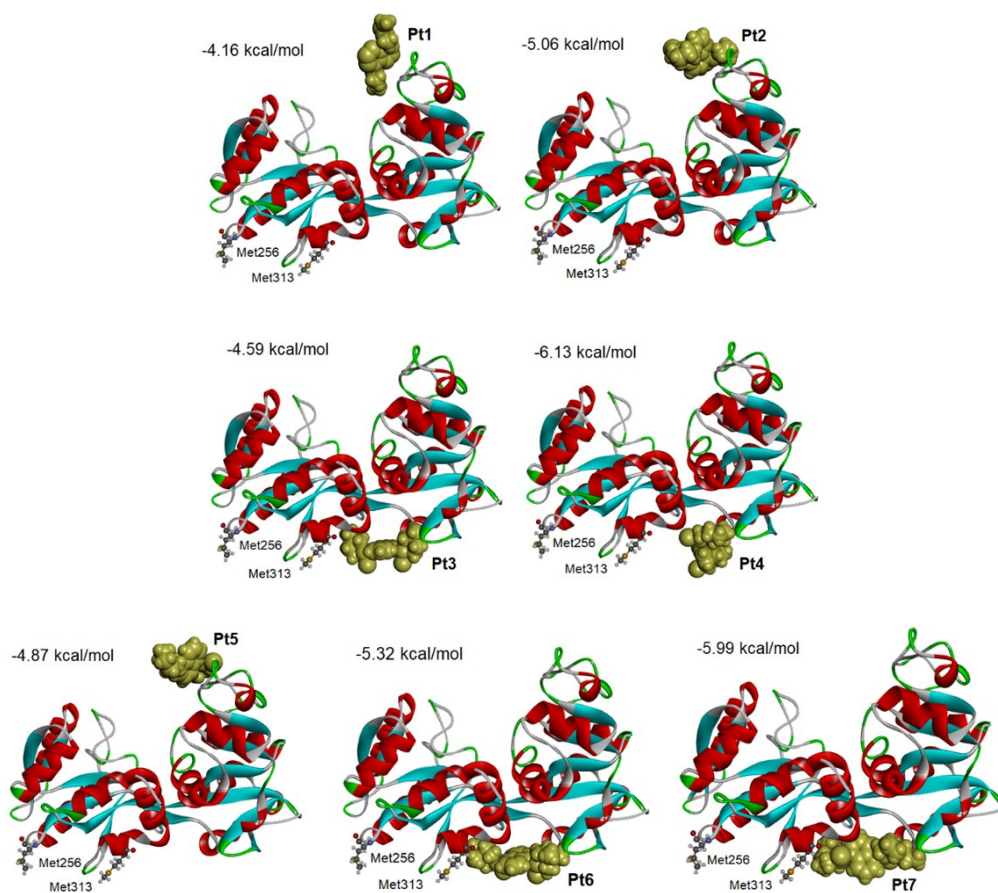


Fig. S6 The structures of the most stable binding modes of dinuclear platinum(II) complexes (**Pt1–Pt7**) to iron-free (apo) form of the recombinant N-lobe of human serum transferrin (ApoTfN), as assessed by molecular docking.

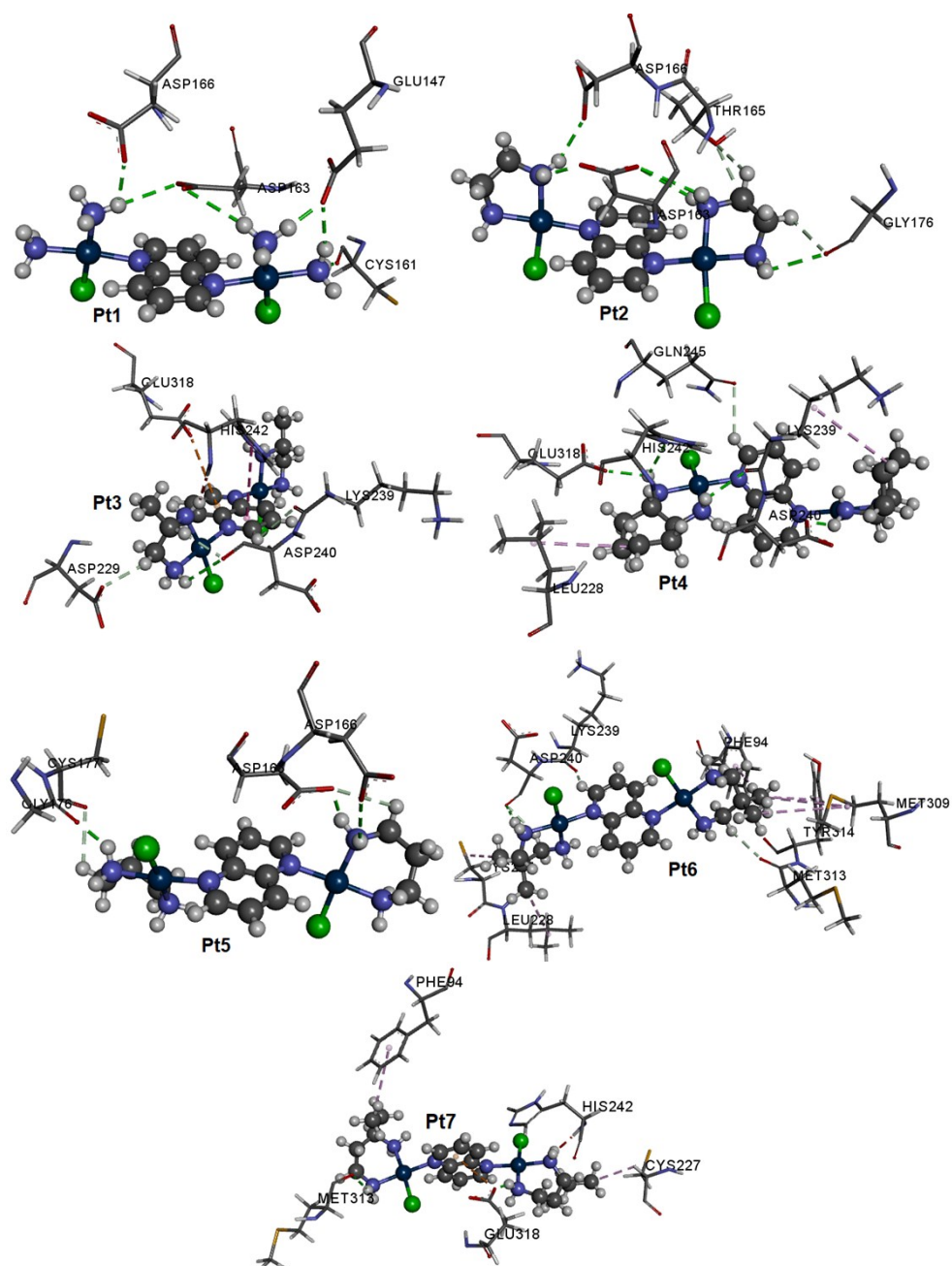


Fig. S7 Amino-acid environment of **Pt1–Pt7** complexes in the most stable orientation of these complexes and iron-free (apo) form of the recombinant N-lobe of human serum transferrin (ApoTfN), as assessed by molecular docking.

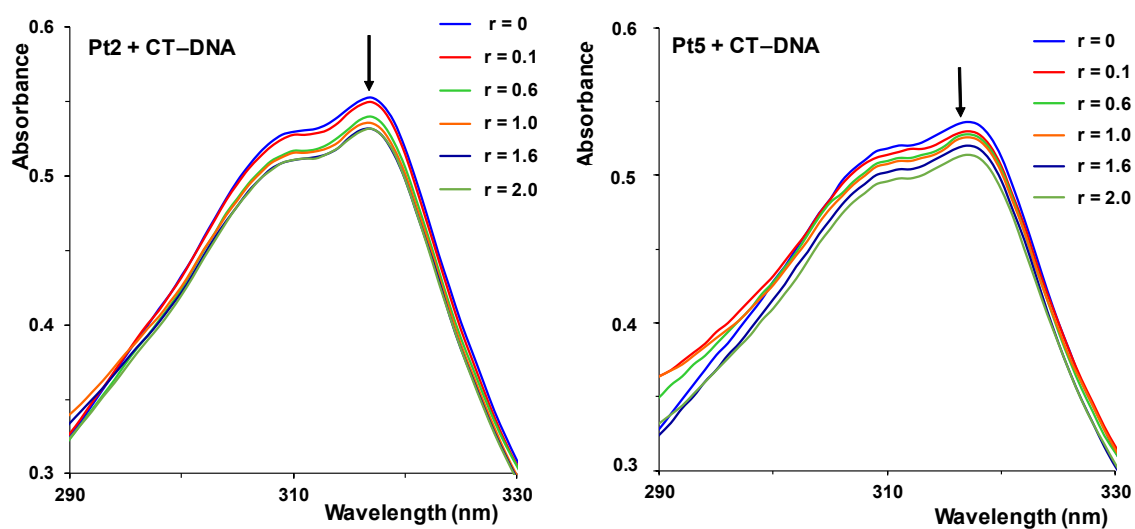


Fig. S8 Absorption spectra of **Pt2** and **Pt5** complexes in the absence and in the presence of increasing amounts of CT-DNA measured in 0.01 M phosphate buffer solution (PBS) at pH 7.40 and 37 °C. $c(\text{Pt(II) complex}) = 8 \mu\text{M}$ ($r = c(\text{DNA})/c(\text{Pt(II) complex}) = 0, 0.1, 0.6, 1.0, 1.6, 2.0$). Arrow shows the absorption intensity changes upon increasing of CT-DNA concentration.

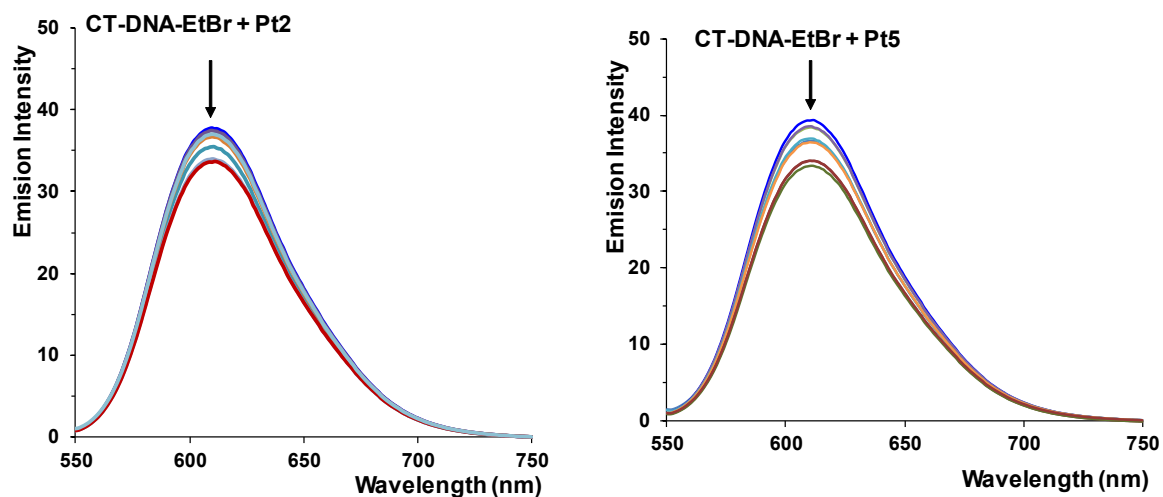


Fig. S9 Emission spectra of the CT-DNA-EtBr system in the absence and in the presence of increasing amounts of **Pt2** and **Pt5** complexes. The spectra were measured in 0.01 M phosphate buffer solution at pH 7.40 and room temperature. $c(\text{EtBr}) = 8 \mu\text{M}$; $c(\text{DNA}) = 8 \mu\text{M}$; $c(\text{Pt(II) complex}) = (0-8) \mu\text{M}$; $\lambda_{\text{ex}} = 527 \text{ nm}$. Arrow shows the emission intensity changes upon increasing of the complex concentration.

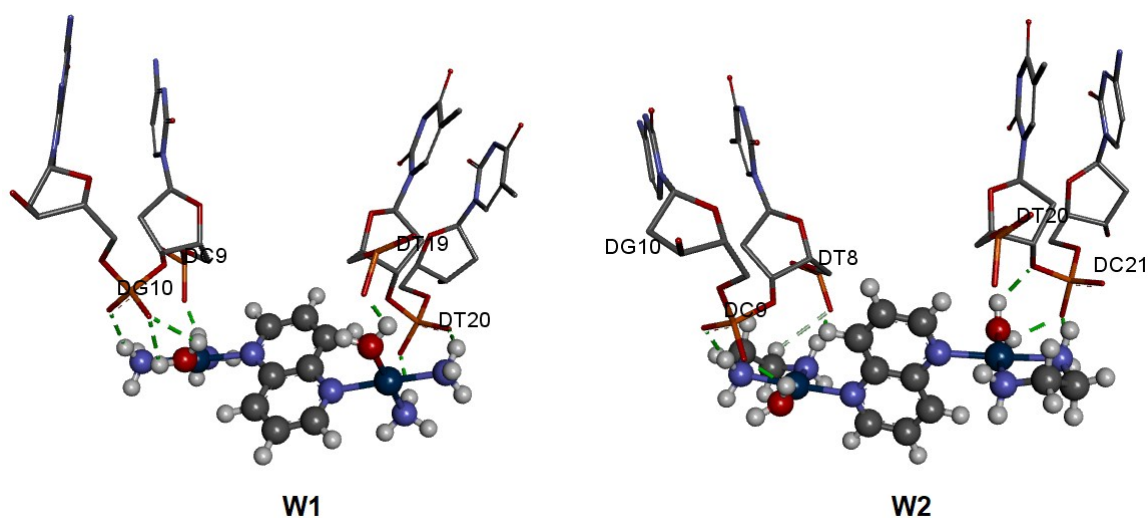


Fig. S10 Binding environments for the most stable binding of aqua complexes **W1** and **W2** to DNA, as assessed by molecular docking (**W1** and **W2** represent aqua derivatives of the corresponding chloride platinum(II) complexes **Pt1** and **Pt2**, respectively).

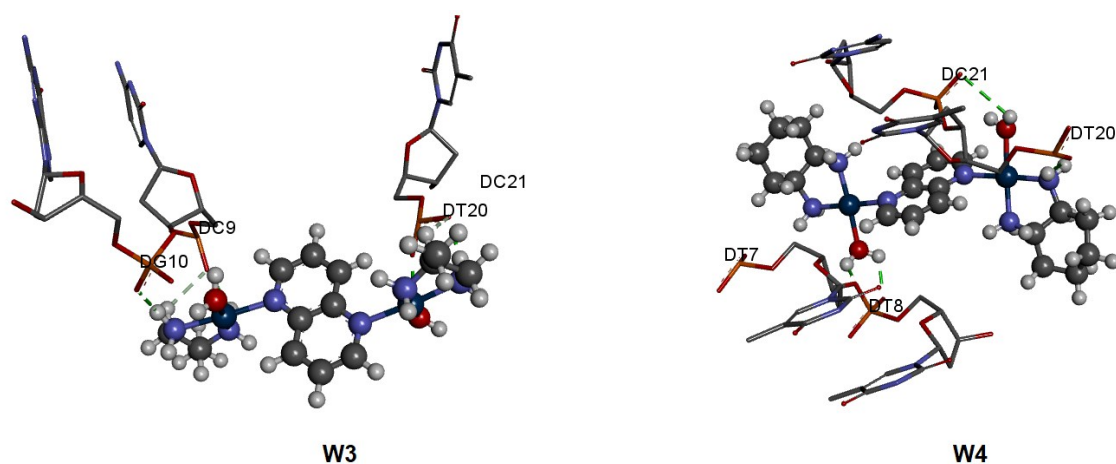


Fig. S11 Binding environments for the most stable binding of aqua complexes **W3** and **W4** to DNA, as assessed by molecular docking (**W3** and **W4** represent aqua derivatives of the corresponding chloride platinum(II) complexes **Pt3** and **Pt4**, respectively).

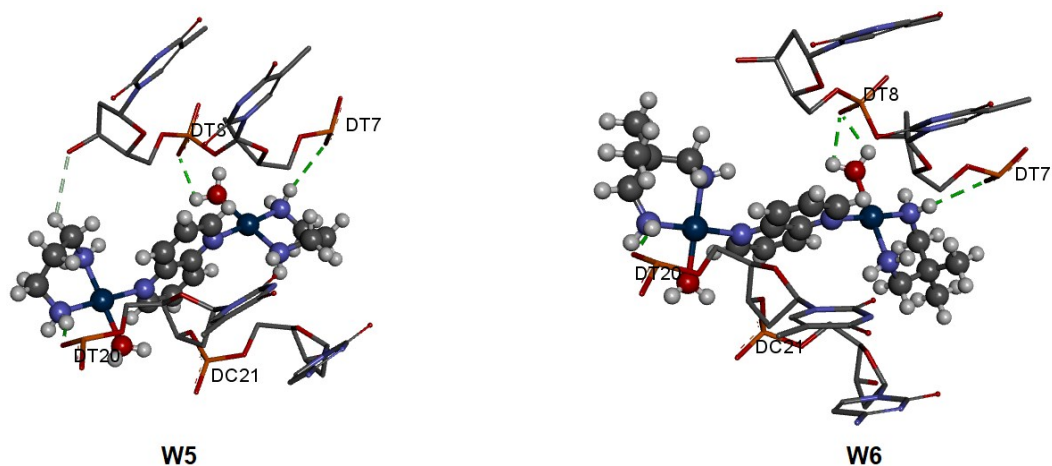


Fig. S12 Binding environments for the most stable binding of aqua complexes **W5** and **W6** to DNA, as assessed by molecular docking (**W5** and **W6** represent aqua derivatives of the corresponding chloride platinum(II) complexes **Pt5** and **Pt6**, respectively).

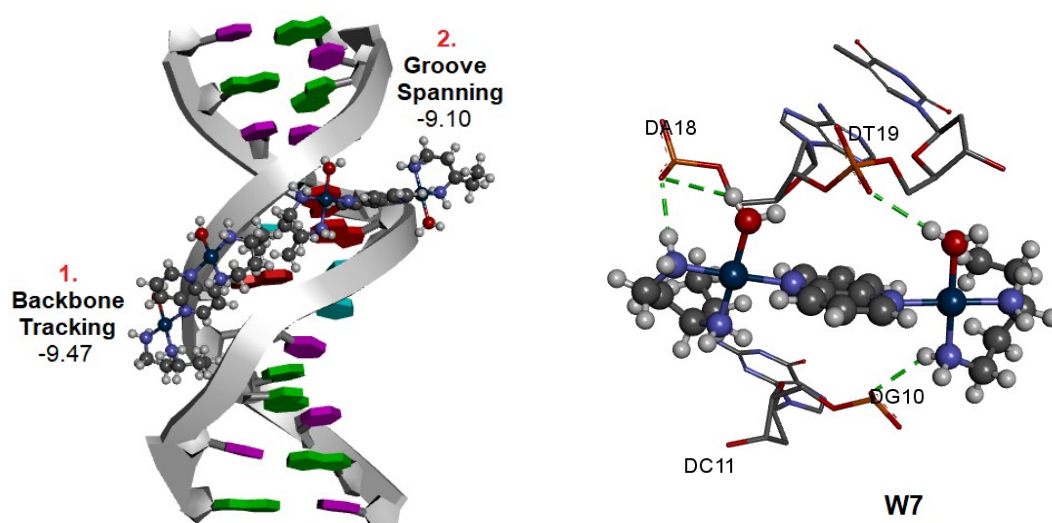


Fig. S13 Two the most stable binding modes and binding environment for the most stable binding mode of platinum(II)-aqua complex **W7** to DNA (backbone tracking), as assessed by molecular docking (**W7** represents aqua derivative of the corresponding chloride platinum(II) complex **Pt7**).

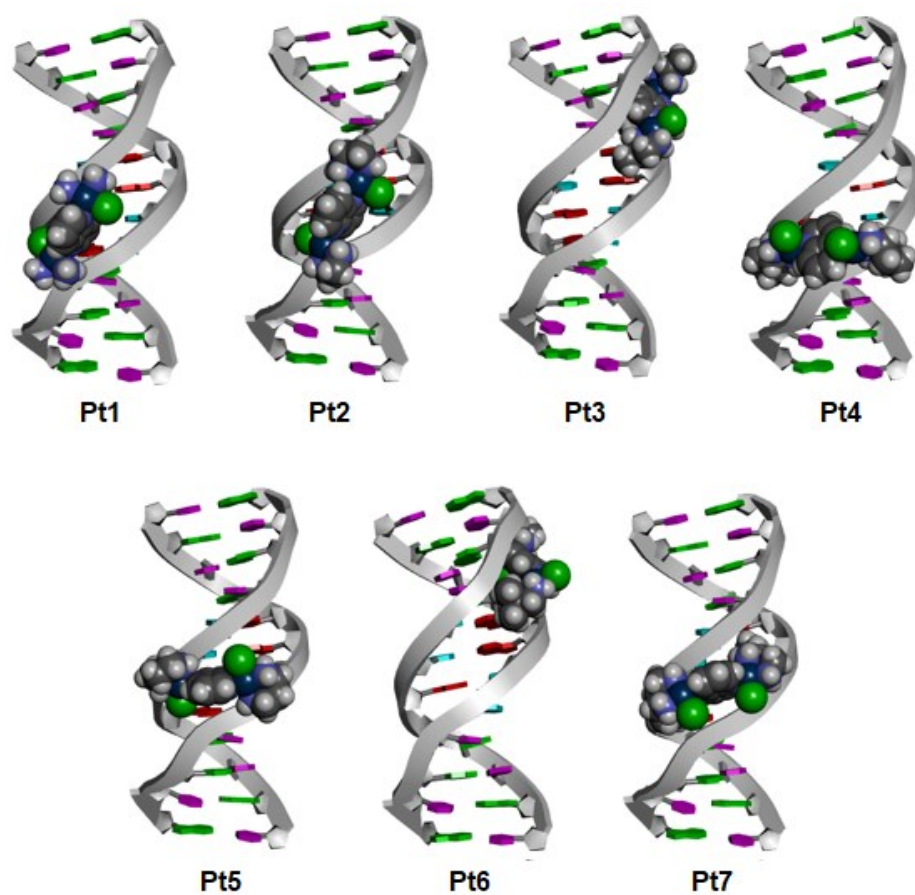
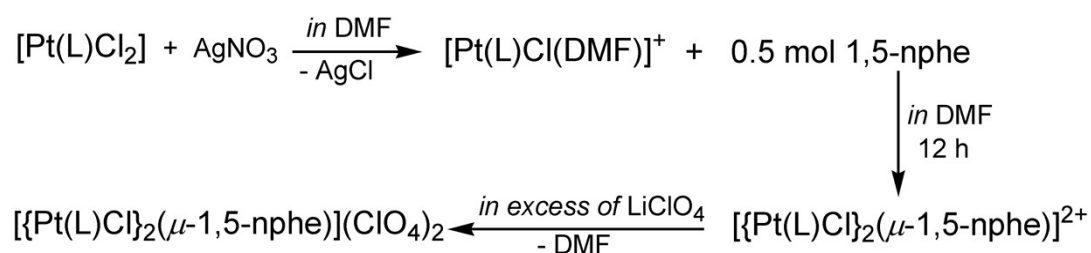


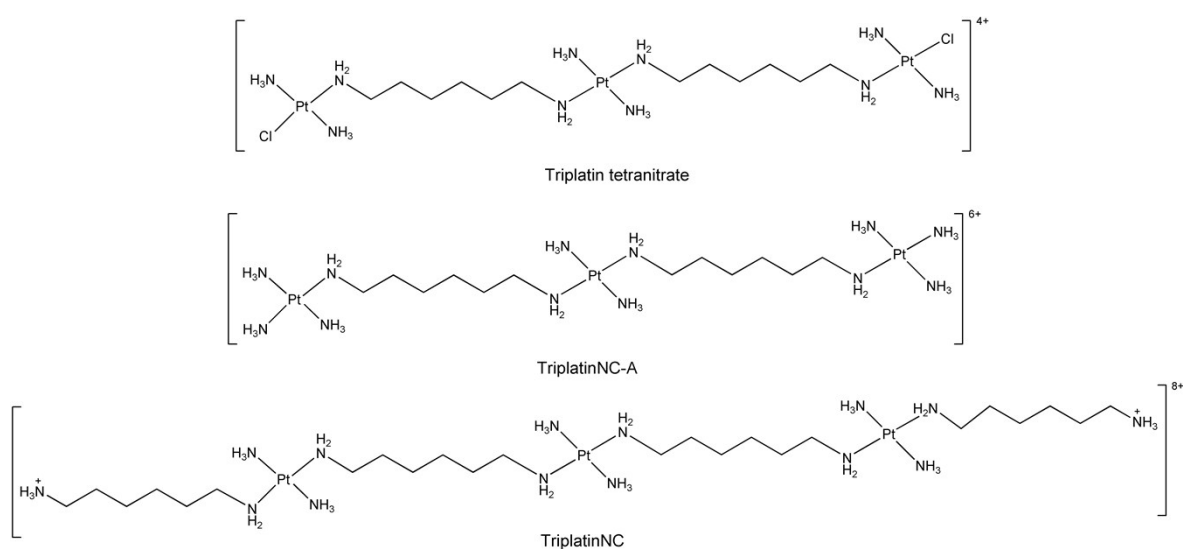
Fig. S14 The structures of the most stable binding modes of dinuclear platinum(II) complexes **Pt1–Pt7** to DNA, as assessed by molecular docking.



Scheme S1 Reaction pathway for preparation of dinuclear platinum(II) complexes **Pt1–Pt7**

(L is 2NH₃ or bidentate coordinated diamine ligand: en, 1,2-pn, dach, 1,3-pd, 2,2-diMe-

1,3-pd and 1,3-pnd; 1,5-nphe is 1,5-naphthyridine).



Scheme S2 Molecular structures of some polynuclear platinum(II) complexes, mentioned

in the main body of the manuscript.